EPJ Appl. Metamat. **11**, 6 (2024)
© S. Amanatiadis et al., Published by EDP Sciences, 2024
https://doi.org/10.1051/epjam/2024009

EPJ Applied Metamaterials

Available online at:
epjam.edp-open.org

Special Issue on 'Metamaterials for Novel Wave Phenomena: Theory, Design and Application in Microwaves', edited by Sander Mann and Stefano Vellucci

Research Article — Open Access

Performance analysis of a novel metamaterial-inspired substrate-integrated cavity for 5G applications

Stamatis Amanatiadis*, Vasileios Salonikios, Nikolaos Kantartzis, and Traianos Yioultsis

Department of Electrical and Computer Engineering, Aristotle University of Thessaloniki, 54124 Thessaloniki, Greece

Received: 30 September 2023 / Accepted: 26 February 2024

Abstract. The functionality of a fully planar metamaterial-inspired substrate-integrated cavity is thoroughly investigated in the present work. The electromagnetic field confinement of the proposed device is realized with the utilization of broadside-coupled complementary split ring resonators that operate as a virtual electric wall. The numerical results from the eigenvalue analysis verify the presence of the fundamental resonances with a noteworthy quality factor. Subsequently, full-wave simulations are conducted to validate the resonance functionality of the proposed device, with excitation achieved using the metallic core of a coaxial cable. Numerical results highlighted, also, the radiation capabilities exploiting the inherent openings in the device due to the complementary resonators.

Keywords: Millimeter-wave / modal analysis / resonator / SIW / SRR

1 Introduction

The establishment of novel technologies in the millimeter-wave regime has been initiated because of the rapid breakthrough of 5G communications. Specifically, the requirement of increased bandwidth forces the telecommunication systems towards higher frequencies where the fabrication procedure is more challenging due to the necessity of finer geometrical characteristics [1]. Additionally, the material and radiation losses in this part of the spectrum exclude various conventional devices of the microwave regime, such as microstrips. For this reason, the concept of the substrate-integrated waveguide (SIW) has been proposed to surpass the majority of these limitations [2,3]. This apparatus consists of a series of conductive via holes that confine the electromagnetic wave, while its operation is equivalent to the bulky metallic waveguides. Moreover, the advantageous aspects of the SIW technology are exploited for the design various embedded components at the mm-wave regime, such antennas [4,5]. One very interesting class of such antennas rely on the utilization of substrate-integrated cavities (SIC) to operate as radiating elements [6–8].

However, the fabrication procedure of the SIW and SIC devices can be cumbersome and costly since the drilling and the metallization injection are required for a considerable number of via holes [1]. Consequently, a fully-planar counterpart has been proposed recently, where the via holes are effectively replaced by metamaterial-inspired elements, particularly broadside-coupled complementary split-ring resonators (BC-CSRR) [9]. In contrast to the physical conductive boundary of the conventional SIW, the BC-CSRRs form a virtual electric field wall that confines the power inside the desired region. Additionally, the resonators are imprinted on the substrate, which facilitates significantly the fabrication procedure, while it retains the ability to integrate components into a single substrate-integrated platform. Specifically, several antenna configurations have been proposed such as a leaky-wave antenna with adjustable main-lobe [9], an H-plane sectoral-horn antenna [10] and a broadband bow-tie [11].

The aforementioned antennas are based on the wave-guiding capability of the BC-CSRR SIW via an aperture adjustment to achieve radiating features. In this paper, we extend the concept of wave confinement using BC-CSRRs to propose a novel fully planar metamaterial-inspired cavity for the millimeter-wave regime. Specifically, the BC-CSRR elements are imprinted in a rectangular shape to confine the electromagnetic field as desired. The proposed device is thoroughly analyzed using a Finite Element Method (FEM) eigenvalue solver to extract its complex eigenfrequencies. Subsequently, the resonance frequencies and their corresponding quality factors are straightforwardly calculated, highlighting remarkable performance for the fundamental one. Finally, full-wave simulations are

* e-mail: samanati@auth.gr

This is an Open Access article distributed under the terms of the Creative Commons Attribution License (https://creativecommons.org/licenses/by/4.0), which permits unrestricted use, distribution, and reproduction in any medium, provided the original work is properly cited.

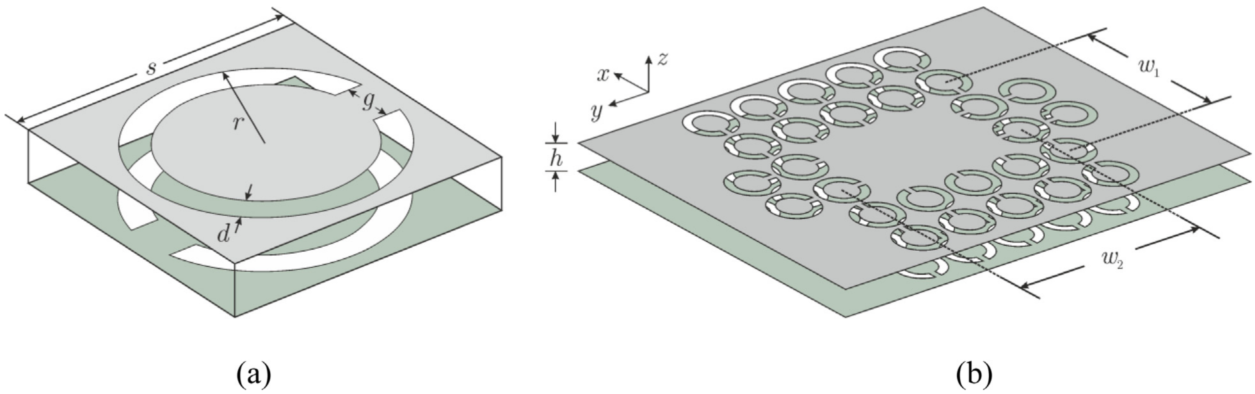

Fig. 1. (a) The unit-cell of the broadside-coupled complementary split-ring resonator and (b) the arrangement of the resonators to form a rectangular cavity.

Table 1. Optimal dimensions for the BC-CSRR SIW at the 5G K-band.

Substrate height h [mm]	Ring radius r [mm]	Rind width d [mm]	Ring gap g [mm]	Unit-cell size s [mm]
0.8	0.84	0.3	0.3	1.88

performed with a Finite-Difference Time-Domain Method (FDTD) to verify the operation as a resonator. Although the potential radiation capability is, also, examined, the primary objective of this work is to serve as a basis for implementing fully-planar cavity antennas utilizing BC-CSRRs.

2 Design of the proposed device

The core element of the proposed device is the BC-CSRR which operates as a virtual electric wall to confine the electromagnetic field. For this reason, its appropriate design is critical for the functionality of the cavity. The unit-cell is depicted in Figure 1a and it consists of a substrate with a metallic coating on both sides, while the split ring resonators are imprinted on the conductors coupled via their broadside. The unit-cell dimensions depend on the frequency spectrum and in this work the K-band is selected to match the 5G 2nd frequency range which extends from 24.25 to 71 GHz. The optimization process focuses on determining the unit cell dimensions necessary for it to act as a single negative material in terms of electric permittivity, enabling its operation as a virtual electric wall. Choosing a substrate with a low dielectric constant and height is crucial to enhancing the coupling between the opposite CSRRs. Any modern optimization algorithm can be employed, with the cost function being the maximization of the negative effective electric permittivity bandwidth. The latter can be straightforwardly evaluated utilizing well-known parameter retrieval techniques [12,13]. This process is thoroughly presented in [9], from which we extract the optimal geometrical characteristics for the K-band, as summarized in Table 1. Note that the dielectric permittivity of the substrate is a typical $\varepsilon_r = 2.2$, while the loss tangent is $\tan\,\delta = 0.001$, corresponding to the low dielectric constant Rogers RT/duroid® 5880.

Then, the metamaterial-inspired cavity is designed with the BC-CSRR elements forming a rectangular region, as illustrated in Figure 1b. Note that two unit-cell series are required on each side of the desired region to properly confine the power, while the cavity size is $w_1 \times w_2$.

3 Modal analysis of the BC-CSRR substrate integrated cavity

The performance analysis of the proposed device is conducted numerically using a 3D FEM eigenvalue solver. It is important to mention that the w_1 gets discrete values to avoid the overlapping or separation of the unit-cells that increase the adjacent cell resonance or become prone to leakage, respectively. Both mechanisms degrade the virtual wall performance and as a consequence the values of w_1 can be $2s$, $3s$,$4s$, etc, controlled by the number of resonators along x-axis, as demonstrated in Figure 1b.

Initially, we design the cavity using three resonators along x-axis leading to $w_1 = 4s \simeq 7.5$ mm. On the other hand, w_2 varies from 2.5 to 4 mm to identify the optimal functionality of the cavity in terms of the resonance frequency and the quality factor. The computational domain is discretized into 311,058 tetrahedrals leading to approximately 2,500,000 degrees of freedom, while the open boundaries are terminated with a scattering condition. The selection of the latter is reasonable since it is expected that the resonances are strongly confined inside the cavity. Finally, the output of the eigensolver is the device's complex eigenfrequencies ω_m, which are converted to the resonance frequency $f_{\rm res}$ and quality factor Q via:

$$f_{\rm res} = \frac{\mathrm{Re}\{\omega_m\}}{2\pi}, \quad Q = \frac{\mathrm{Re}\{\omega_m\}}{\mathrm{Im}\{\omega_m\}}. \tag{1}$$

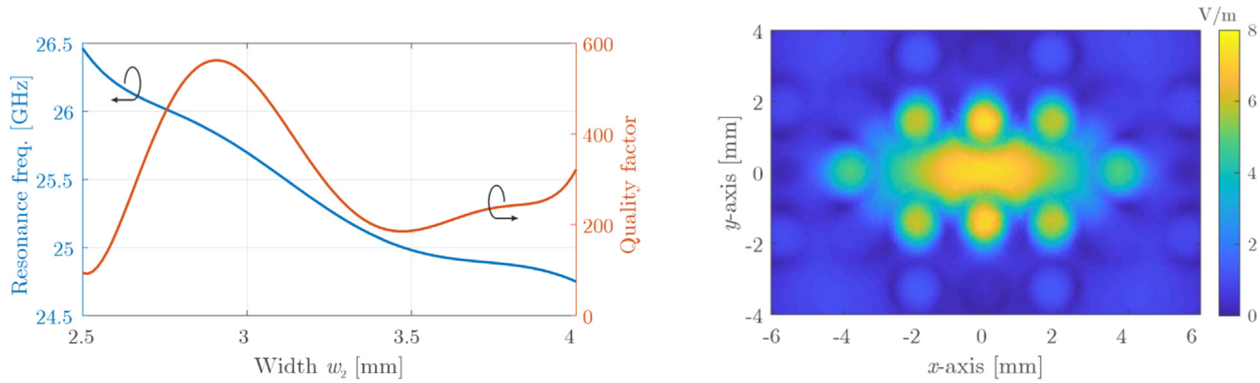

(a) (b)

Fig. 2. Resonance frequency and quality factor versus the width w_2 and (b) electric field distribution for $w_2 = 2.8$ mm of the proposed cavity's first mode TE_{110}.

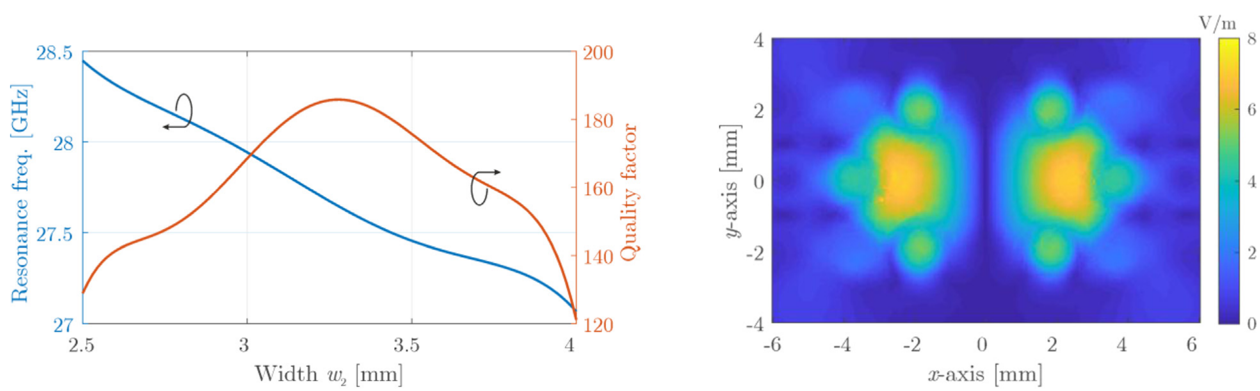

(a) (b)

Fig. 3. Resonance frequency and quality factor versus the width w_2 and (b) electric field distribution for $w_2 = 3.5$ mm of the proposed cavity's first mode TE_{210}.

The extracted results for the fundamental mode, i.e., TE_{110}, are depicted in Figure 2a, where it is evident that the optimal performance appears for $w_2 = 2.8$ mm since the maximum value of the quality factor is detected, particularly 580. The resonance frequency for this value is approximately 26 GHz and the distribution of its electric field is demonstrated in Figure 2b. Here, the confinement of the electric field inside the cavity is verified with the intensity maximized at its center. Moreover, the value is independent to the z-axis, i.e., the normal of the cavity plane, verifying the formation of the TE_{110} mode since the electric field is minimized near the virtual electric wall. It is worth observing that although the quality factor is increased over $w_2 = 3.8$ mm, the resonance is mainly confined to the BC-CSRRs instead of the cavity itself; therefore, the desired functionality is absent.

Furthermore, the second mode, i.e., TE_{210}, is investigated and its attributes are sketched in Figure 3a highlighting a smoother performance of the quality factor for the range 27−28 GHz. However, its value is almost a quarter of the first mode. Additionally, the electric field distribution is illustrated in Figure 3b for $w_2 = 3.5$ mm indicating the two oscillation towards x-axis.

As mentioned previously, the w_1 values are discrete to avoid the resonator degradation. Now, various of these values are compared in terms of the resonance frequency and the quality factor concerning the TE_{110} mode. The results for the resonance frequency are sketched in Figure 4a, indicating the same trend, but increased values for lower w_1. However, the quality factor, in Figure 4b, highlights that the optimal value is observed for different w_2 arrangement. The most advantageous performance is observed for the previously analysed $w_1 \simeq 7.5$ mm, while the most compact one with $w_1 \simeq 3.8$mm has a maximum quality factor 570 at 26.4 GHz for $w_2 = 3.6$ mm.

Finally, the performance of the proposed cavity is compared with the equivalent SIC with metallic via holes. The functionality of the latter is identical to a dielectric-filled cavity with metallic boundaries. As a consequence, the resonance frequency and the quality factor, considering

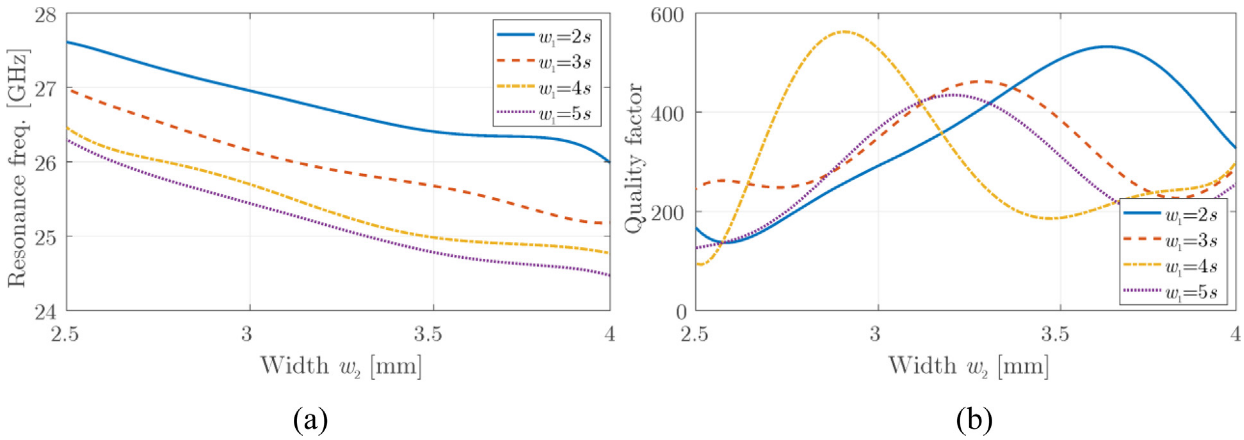

Fig. 4. (a) Resonance frequency and (b) quality factor comparison for the TE_{110} mode of cavities with different discrete w_1 values.

Table 2. Performance comparison between a conventional SIC with metallic via-holes and the proposed BC-CSRR based one.

Cavity type	Dimensions [mm]	Resonance frequency [GHz]	Quality factor
Conventional SIC	9.5×4.3	26	1000
Proposed BC-CSRR SIC	13.2×8.4	26	580

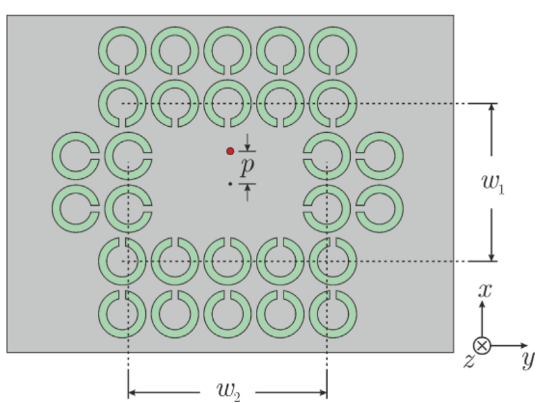

Fig. 5. The BC-CSRR substrate integrated cavity antenna.

negligible conductivity losses, is theoretically determined via:

$$f_{\mathrm{res}}^{110} = \frac{c_0}{2\sqrt{\varepsilon_r}}\sqrt{\frac{1}{w_1^2}+\frac{1}{w_2^2}}, \quad Q = \frac{1}{\tan\delta}, \tag{2}$$

where the dimensions w_1 and w_2 are the corresponding ones of Figure 1b since the substrate height is considerably lower and the dielectric properties are identical to the proposed device ($\varepsilon_r = 2.2$, $\tan\delta = 0.001$). The comparison is demonstrated in Table 2, where it is evident that the proposed device achieves the same resonance frequency with somewhat increased dimensions and decreased quality factor. However, these aspects come as a trade-off for the advantage of avoiding the via hole drilling since the proposed BC-CSRR cavity is fully planar.

4 Design verification via full-wave simulations

The previous modal analysis of the metamaterial-inspired cavity highlighted the tuning of the resonance frequencies at the K-band of the 5G spectrum. Now, a full-wave analysis is conducted using an excitation that stimulates the dominant mode of the cavity, as depicted in Figure 5. Specifically, a realistic implementation of the source includes the core of a coaxial cable at distance p from the cavity centre towards the long side, while the shielding of the cable can be attached on the ground-plane. Although the cavity antennas require an opening to radiate efficiently, the parasitic radiation of the resonators can be exploited for this particular setup.

The considered cavity for the full-wave simulations has identical dimensions with the one of the modal analysis, namely $w_1 = 7.5$ mm with varying w_2. However, the position p of the excitation has a crucial role for the optimized stimulation of the cavity. The influence of this displacement is evaluated in Figure 6, where different stimulation locations are considered for the case with the higher quality factor, i.e., for $w_2 = 2.8$ mm. Here, it is evident that the stronger resonance is observed for $p = 0.8$ mm. On the other hand, this distance is increased to $p = 1$ mm, $p = 2$ mm and $p = 2.5$ mm for $w_2 = 2.9$ mm, $w_2 = 3$ mm and $w_2 = 3.1$ mm, respectively. Note that for even larger w_2, the optimal value for the displacement is retained at 2.5 mm.

All the numerical results in this paper are extracted via the efficient FDTD method. Note that the conventional staircase algorithm is enhanced via the numerically stable conformal modelling technique of [14] to accurately design the curved metallic regions of the resonators. The computational domain is divided into $100 \times 80 \times 60$

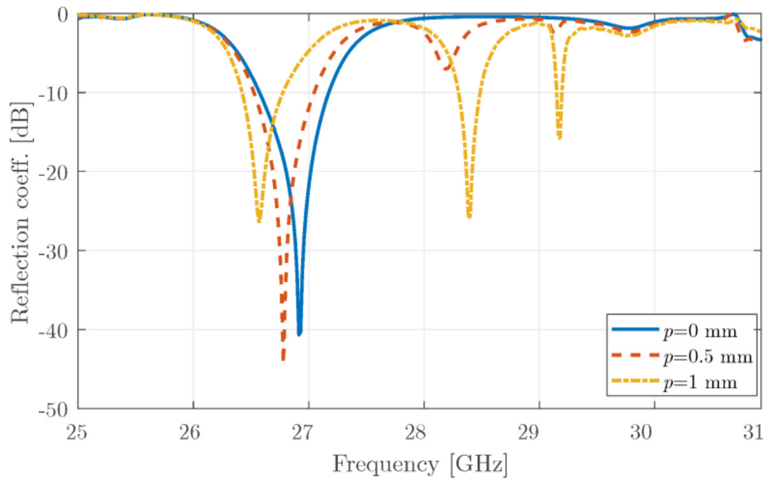

Fig. 6. Reflection coefficient of the proposed cavity for w_1 = 7.5 mm, w_2 = 2.8 mm and different stimulation locations.

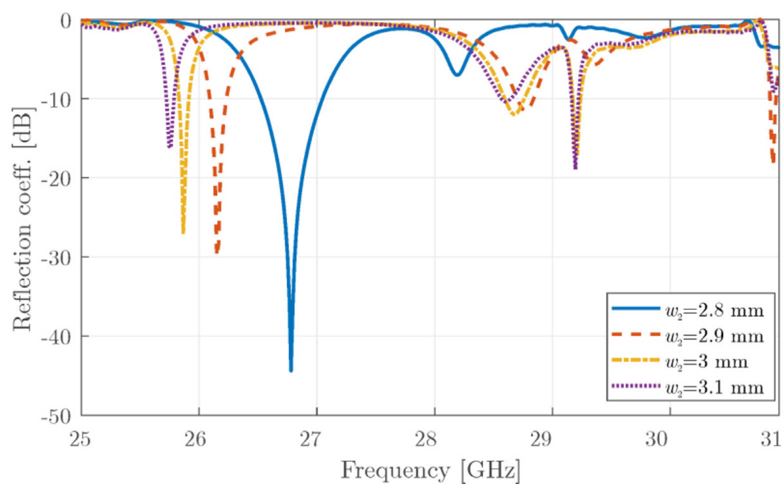

Fig. 7. Reflection coefficient of the proposed cavity for w_1 = 7.5 mm and various w_2 values.

mesh-cells of mean size $\Delta = 0.25$ mm. The time-step is selected at 0.48 ps to ensure the simulation stability, while a broadband pulse excitation is utilized at the frequency range 20–35 GHz. Finally, the open boundaries are truncated via an 8-cell thick Perfectly Matched Layer to effectively absorb the outgoing waves.

Bearing in mind the above-mentioned features, the reflection coefficient is illustrated in Figure 7 for various values of w_2 (retaining w_1 = 7.5 mm), using the optimal position of the excitation. Here, it is evident that the enhanced functionality of the cavity is achieved for w_2 = 2.8 mm, which is successfully predicted by the modal analysis. Nevertheless, the exact location of the resonance is somewhat shifted towards higher frequencies for all the cases. One possible explanation for this behaviour is the fact the virtual electric wall of the BC-CSRRs has no strict limits for the electric field minimization in contrast to the physical conductive via holes.

Finally, the electric field distribution is examined in Figure 8a for the optimal case, namely the one with w_2 = 2.8 mm. Here, it is evident that the energy is confined, mainly, inside the cavity through the activation of the resonators; thus, the resonating functionality is verified. Nevertheless, the examined device is acting, also, as a radiator since the complementary resonators are operating as apertures. Although this is a parasitic behaviour for waveguiding purposes, it is exploited for the proposed cavity to offer antenna capabilities without the need of additional openings. For this reason, the radiation properties are not the expected for the TE_{110} cavity mode, but exhibit four lobes towards the small short sides of the cavity, demonstrated in the 3D radiation pattern at the resonance frequency of Figure 8b. The maximum of the radiation is observed at the upper side of the substrate with a directivity that approaches 5 dBi, while the efficiency is calculated 99,97%. As a result, the realized gain closely aligns with the directivity values, given the minimal

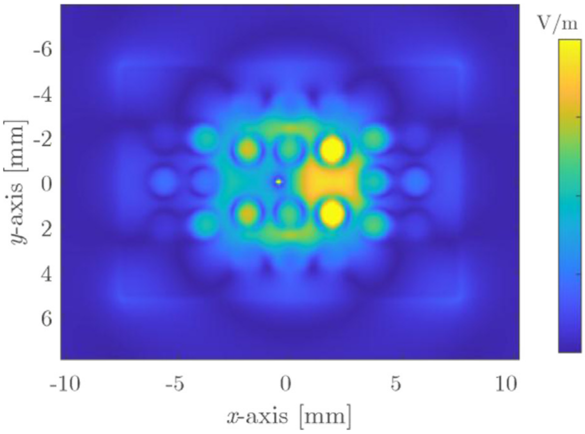

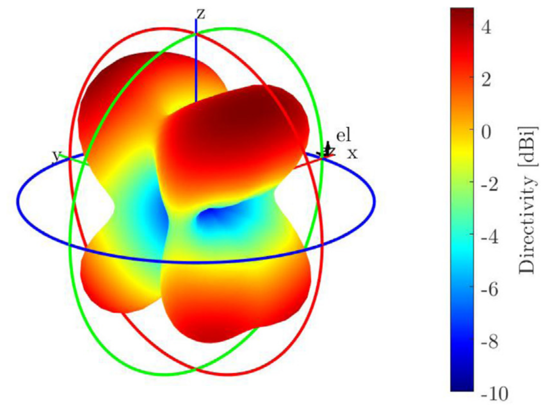

Fig. 8. (a) Electric field distribution and (b) 3D radiation pattern extracted by full-wave analysis of the proposed cavity antenna for w_1=7.5 mm and w_2 = 2.8 mm.

mismatch losses and the high efficiency. It's essential to emphasize that the evaluated radiation features emerge as a side-effect of the cavity design. Therefore, more sophisticated approaches are required to optimally exploit the BC-CSRR SIC as a cavity antenna. Note that despite initial concerns about the size of the device when combining an array with cavities for beamforming capabilities, the same resonators can be used for the adjacent cavities to effectively reduce the overall dimensions.

5 Conclusion

A fully-planar metamaterial-inspired substrate-integrated cavity has been designed and thoroughly investigated in the present work. The confinement of the field inside the cavity has been realized by the virtual electric wall that is formed with the broadside-coupled complementary split-ring resonators. The eigenvalue analysis highlighted a notable performance of the fundamental mode, while the full-wave simulation verified the resonance functionality of proposed cavity that can, also, operate as an easy-to-fabricate antenna for 5G applications.

Funding

The research project was supported by the Hellenic Foundation for Research and Innovation (H.F.R.I.) under the "2nd Call for H.F.R.I. Research Projects to support Post-Doctoral Researchers" (Project Number: 756).

Conflict of interest

The authors declare no conflict of interest.

Data availability statement

The data presented in this study are available upon request from the corresponding author (samanati@auth.gr).

Author contribution statement

S. Amanatiadis: Conceptualization, Methodology, Formal analysis, Project administration, Writing–original draft preparation. V. Salonikios: Investigation, Validation. N. Kantartzis and T. Yioultsis: Supervision, Writing–review and editing.

References

1. Z.A. Bhat, J.A. Sheikh, R. Rehman, S.D. Khan, I. Bashir, S. Ashraf, A survey on substrate integrated waveguide filters; design challenges and miniaturizing techniques for the 5G, Int. J. High Speed Electr. Syst. **32**, 2140006 (2023)
2. D. Deslandes, K. Wu, Accurate modeling, wave mechanisms, and design considerations of a substrate integrated waveguide, IEEE Trans. Microwave Theory Tech. **54**, 2516 (2006)
3. M. Bozzi, A. Georgiadis, K. Wu, Review of substrate-integrated waveguide circuits and antennas, IET Microw. Antennas Propag. **5**, 909 (2011)
4. S. Mukherjee, A. Biswas, Design of self-diplexing substrate integrated waveguide cavity-backed slot antenna, IEEE Antennas Wireless Propag. Lett. **15**, 1775 (2016)
5. Q. Zhu, K.B. Ng, C.H. Chan, K.M. Luk, Substrate-integrated-waveguide-fed array antenna covering 57–71 GHz band for 5G applications, IEEE Trans. Antennas Propag. **65**, 6298 (2017)
6. Q. Liu, L. Zhu, J. Wang, W. Wu, A wideband patch and SIW cavity hybrid antenna with filtering response, IEEE Antennas Wireless Propag. Lett. **19**, 836 (2020)
7. R. Lu, C. Yu, Y. Zhu, X. Xia, W. Hong, Millimeter-wave dual-band dual-polarized SIW cavity-fed filtenna for 5G applications, IEEE Trans. Antennas Propag. **70**, 10104 (2022)
8. E. Aparna, G. Ram, G.A. Kumar, Review on substrate integrated waveguide cavity backed slot antennas, IEEE Access **10**, 133504 (2022)
9. M. Nitas, M.T. Passia, T.V. Yioultsis, Fully planar slow-wave substrate integrated waveguide based on broadside-coupled complementary split ring resonators for mmWave and 5G components, IET Microw. Antennas Propag. **14**, 1096 (2020)
10. V. Salonikios, M. Nitas, S. Raptis, T.V. Yioultsis, Design of a fully planar BC-CSRR SIW-based H-plane sectoral horn with a printed transition, in *2019 13th European Conference on Antennas and Propagation* (*EuCAP*) (2019), pp. 1–5
11. C. Feng, T. Shi, L. Wang, Novel broadband bow-tie antenna based on complementary split-ring resonators enhanced substrate-integrated waveguide, IEEE Access **7**, 12397 (2019)
12. X. Chen, T.M. Grzegorczyk, B.I. Wu, J. Pacheco Jr, J.A. Kong, Robust method to retrieve the constitutive effective parameters of metamaterials, Phys. Rev. E **70**, 016608 (2004)

13. D.R. Smith, D.C. Vier, T. Koschny, C.M. Soukoulis, Electromagnetic parameter retrieval from inhomogeneous metamaterials, Phys. Rev. E **71**, 036617 (2005)
14. S. Dey, R. Mittra, A modified locally conformal finite-difference time-domain algorithm for modeling three-dimensional perfectly conducting objects, Microwave Opt. Technol. Lett. **17**, 349 (1998)

Cite this article as: Stamatis Amanatiadis, Vasileios Salonikios, Nikolaos Kantartzis, Traianos Yioultsis, Performance analysis of a novel metamaterial-inspired substrate-integrated cavity for 5G applications, EPJ Appl. Metamat. **11**, 6 (2024)